Vibrational Spectroscopic Analysis of Taranakite $(K,NH_4)Al_3(PO_4)_3(OH) \cdot 9(H_2O)$ from the Jenolan Caves, Australia

Ray L. Frost,[1] • Yunfei Xi,[1] Sara J. Palmer[1] and Ross Pogson[2]

[1]Chemistry Discipline, Faculty of Science and Technology, Queensland University of Technology, GPO Box 2434, Brisbane Queensland 4001, Australia.

[2] Mineralogy & Petrology, Australian Museum, 6 College St., Sydney, NSW, Australia 2010

Abstract

Many phosphate containing minerals are found in the Jenolan Caves. Such minerals are formed by the reaction of bat guano and clays from the caves. Among these cave minerals is the mineral taranakite $(K,NH_4)Al_3(PO_4)_3(OH)\cdot 9(H_2O)$ which has been identified by X-ray diffraction. Jenolan Caves taranakite has been characterised by Raman spectroscopy. Raman and infrared bands are assigned to $H_2PO_4^-$, OH and NH stretching vibrations. By using a combination of XRD and Raman spectroscopy, the existence of taranakite in the caves has been proven.

Keywords: Raman spectroscopy, infrared spectroscopy, cave minerals, phosphate, taranakite, brushite

• Author to whom correspondence should be addressed (r.frost@qut.edu.au)

Introduction

The mineral taranakite $(K,NH_4)Al_3(PO_4)_3(OH)\cdot 9H_2O$ is a well known cave mineral [1-6]. The mineral was first discovered in the Minerva caves in France in 1894. The mineral is named after the Taranaki district in New Zealand and is an alkali alumina phosphate formed from the reaction of bat or bird guano with clays or aluminous rocks. Taranakite is most commonly found in humid, bat inhabited caves near the boundary of guano layers with the cave surface. It is also found in perennially wet coastal locations that have been occupied by bird colonies. Taranakite forms small white, pale yellow or gray crystals, which are typically found in pulverulent nodular aggregates, or crusts. The mineral was described in 1898 as minervite in the Jenolan Caves but the mineral was not defined. The objective of this research is to positively identify the mineral in samples taken from the Jenolan Caves.

Taranakite crystallizes in the hexagonal system, and is noted as having the longest crystallographic axis of any known mineral: the *c*-axis of the taranakite unit cell is 9.505 nanometres long [7, 8]. According to Dick et al. X-ray crystal data are space group R$\underline{3}$c , a 870.25(11), c 9505.(1) pm, Z = 6, Rg = 0.028. Dick et al. also provided neutron scattering data with subsequent Rietveld refinement of the powder pattern of deuterated taranakite elucidated the D-atom positions. Neutron crystal data were found to be a 868.82(3), c 9498.(2) pm, Rwp = 0.061. Taranakite is a layer structured mineral having six layers $[K_3Al_5(HPO_4)6(PO_4)_2(H_2O)_{12}]$ separated from each other by H_2O layers. According to these authors the rigid layer is formed by columns of corner sharing H phosphate tetrahedra and Al octahedra which are interconnected by additional six-coordinated Al ions. In trigonal holes of the layer orthophosphate ions are situated n-onexchangeable K ions trapped within the layers. H bonds in taranakite are formed between building units within the rigid layer, within the H_2O interlayer, and between layer and interlayer.

Raman spectroscopy has proven very useful for the study of minerals [9-17]. Indeed Raman spectroscopy has proven most useful for the study of diagentically related minerals as often occurs with minerals containing phosphate groups as may be found in cave systems. This paper is a part of systematic studies of vibrational spectra of minerals of secondary origin in the oxide supergene zone [13-15, 18-23]. In this work we attribute bands at various

wavenumbers to vibrational modes of taranakite using Raman spectroscopy and relate the spectra to the structure of the mineral.

Experimental

Minerals

The mineral taranankite (D58072) was sourced from The Australian Museum and originated from the Jenolan Caves, New South Wales, Australia. The particular cave where the mineral was found is called the Katies Bower of the Chifley Cave system. Taranakite occurs as soft, white flour-like powders in the Jenolan Caves. The mineral has been analysed and the data published [24]. The mineral has been identified in many cave systems worldwide [1-3, 5, 6, 25-27].

X-ray diffraction

The cave mineral taranakite was powdered and X-ray diffraction patterns were collected using a Philips X'pert wide angle X-Ray diffractometer, with Cu Kα radiation (1.54052 Å).

Raman spectroscopy

Crystals of taranakite were placed on a polished metal surface on the stage of an Olympus BHSM microscope, which is equipped with 10x, 20x, and 50x objectives. The microscope is part of a Renishaw 1000 Raman microscope system, which also includes a monochromator, a filter system and a CCD detector (1024 pixels). The Raman spectra were excited by a Spectra-Physics model 127 He-Ne laser producing highly polarised light at 633 nm and collected at a nominal resolution of 2 cm^{-1} and a precision of ± 1 cm^{-1} in the range between 100 and 4000 cm^{-1}. Repeated acquisition on the crystals using the highest magnification (50x) was accumulated to improve the signal to noise ratio in the spectra. Spectra were calibrated using the 520.5 cm^{-1} line of a silicon wafer.

Infrared spectroscopy

Infrared spectra were obtained using a Nicolet Nexus 870 FTIR spectrometer with a smart endurance single bounce diamond ATR cell. Spectra over the 4000–525 cm^{-1} range were

obtained by the co-addition of 128 scans with a resolution of 4 cm^{-1} and a mirror velocity of 0.6329 cm/s. Spectra were co-added to improve the signal to noise ratio.

Band component analysis was undertaken using the Jandel 'Peakfit' (Erkrath, Germany) software package which enabled the type of fitting function to be selected and allowed specific parameters to be fixed or varied accordingly. Band fitting was done using a Lorentz-Gauss cross-product function with the minimum number of component bands used for the fitting process. The Lorentz-Gauss ratio was maintained at values greater than 0.7 and fitting was undertaken until reproducible results were obtained with squared correlations (r^2) greater than 0.995. Band fitting of the spectra is quite reliable providing there is some band separation or changes in the spectral profile.

Results and discussion

X-ray diffraction

The X-ray diffraction patterns of the Jenolan Caves taranakite sample together with the standard reference patterns of taranakite and variscite are displayed in Figure 1. Clearly the sample contains taranakite as the principal phase and with a minor phase of variscite. The formula of taranakite is given as $(K,NH_4)Al_3(PO_4)_3(OH)\cdot 9H_2O$. The structure as reported by Dick et al. [7] clearly indicates that the mineral contains hydrogen phosphate units. Thus the formula should be written as $(K,NH_4)Al_3(PO_4)_2(HPO_4)\cdot 9H_2O$. The mineral also may contain Na as a substitution for the NH_4^+ anion. Some substitution of Al^{3+} by Fe^{3+} may also occur.

Vibrational spectroscopy background

In aqueous systems, the Raman spectra of phosphate oxyanions show a symmetric stretching mode (ν_1) at 938 cm^{-1}, an antisymmetric stretching mode (ν_3) at 1017 cm^{-1}, a symmetric bending mode (ν_2) at 420 cm^{-1} and a ν_4 bending mode at 567 cm^{-1} [28-30]. S.D. Ross in Farmer (page 404) listed some well-known minerals containing phosphate which were either hydrated or hydroxylated or both [31]. The vibrational spectrum of the dihydrogen phosphate anion has been reported in Farmer. The PO_2 symmetric stretching mode occurs at 1072 cm^{-1} and the POH symmetric stretching mode at ~878 cm^{-1}. The POH antisymmetric stretching mode was at 947 cm^{-1} and the $P(OH)_2$ bending mode at 380 cm^{-1}. The band at 1150 cm^{-1} was

assigned to the PO_2 antisymmetric stretching mode. The position of these bands will shift according to the crystal structure of the mineral.

The vibrational spectra of phosphate minerals has been published by S. D. Ross in Farmer's treatise Chapter 17 [31]. The Table 17.III reports the band positions of a wide range of phosphates and arsenates [31]. The band positions for the monohydrogen phosphate anion of disodium hydrogen phosphate dihydrate is given as ν_1 at 820 and 866 cm^{-1}, ν_2 at around 460 cm^{-1}, ν_3 as 953, 993, 1055, 1070, 1120 and 1135 cm^{-1}, ν_4 at 520, 539, 558, 575 cm^{-1}. The POH unit has vibrations associated with the OH specie. The stretching vibration of the POH units was tabulated as 2430 and 2870 cm^{-1}, and bending modes at 766 and 1256 cm^{-1}. Water stretching vibrations were found at 3050 and 3350 cm^{-1}. The position of the bands for the disodium hydrogen phosphate is very dependent on the waters of hydration. There have been several Raman spectroscopic studies of the monosodium dihydrogen phosphate chemicals [32-36].

Spectroscopy

The Raman spectrum of taranakite in the 700 to 1200 cm^{-1} region and infrared spectrum in the 500 to 1300 cm^{-1} region are displayed in Figures 2a and 2b respectively. Intense Raman bands are observed at 962 and 1126 cm^{-1}. Other low intensity bands are observed at 922, 946, 1010, 1026, 1041, 1064, 1100 and 1149 cm^{-1}. The observation of multiple low intensity bands suggests the presence of other phosphate minerals in the Jenolan Caves sample.
The Raman band at 962 cm^{-1} is assigned to the ν_1 symmetric stretching mode of the POH units, whereas the Raman band at 1010 cm^{-1} is assigned to the ν_1 symmetric stretching mode of the PO_4^{3-} units. Galy [34] first studied the polarized Raman spectra of the $H_2PO_4^-$ anion. Choi *et al.* reported the polarization spectra of NaH_2PO_4 crystals. Casciani and Condrate [37] published spectra on brushite and monetite together with synthetic anhydrous monocalcium phosphate ($Ca(H_2PO_4)_2$), monocalcium dihydrogen phosphate hydrate ($Ca(H_2PO_4)_2 \cdot H_2O$) and octacalcium phosphate ($Ca_8H_2(PO_4)_6 \cdot 5H_2O$). These authors determined band assignments for $Ca(H_2PO_4)$ and reported bands at 1002 and 1011 cm^{-1} as POH and PO stretching vibrations, respectively. The two Raman bands at 1139 and 1165

cm^{-1} are attributed to both the HOP and PO antisymmetric stretching vibrations. Casciani and Condrate [37] tabulated Raman bands at 1132 and 1155 cm^{-1} and assigned these bands to P-O symmetric and the P-O antisymmetric stretching vibrations. The first assignment, however, differs from what is stated in this work.

The infrared spectrum displays greater complexity with multiple overlapping bands (Figure 2b). The complexity of the spectrum makes it difficult to undertake band assignments. This complexity may be due to a mixture of taranakite and variscite. There is a difference between taking a Raman spectrum and an infrared spectrum. The sample spot size of the Raman spectrometer is around 1 micron. In infrared spectroscopy the measurement size is at best 30 microns. Thus in Raman spectroscopy it is possible to collect data for a pure mineral because that crystal was selected. It is more likely that the infrared spectrum is more likely to collect data for a mixture. This is why of course it is an advantage to run the Raman spectrum. Intense infrared bands are observed at 1016, 1059 and 1100 cm^{-1}. Other strong bands are observed at lower wavenumbers than these intense bands at 826, 875, 909, 948 and 966 cm^{-1}. On the higher wavenumber side, infrared bands are found at 1121, 1149, 1191, 1224 and 1280 cm^{-1}. The intense band at 1016 cm^{-1} is attributed to the PO_4^{3-} symmetric stretching mode and the two bands at 1059 and 1100 cm^{-1} to the PO_4^{3-} antisymmetric stretching mode. The bands at 909, 948 and 966 cm^{-1} are associated with the stretching vibrations of $HOPO_3^{2-}$ units. Infrared bands for the mineral dittmarite $(NH_4)MgPO_4 \cdot H_2O$ are found at 978, 1063 and 1105 cm^{-1} (this work). Choi *et al.* [33] published spectra of NaH_2PO_4; however these authors did not tabulate or mark the position of the peaks. Therefore, it is very difficult to make any comparison of the peak positions of archerite and that of published data by Choi *et al.* Casciani and Condrate [37] reported bands assigned to these vibrational modes for $Ca(H_2PO_4)_2$ at 876 and 901 cm^{-1}. The infrared bands at 728, 826 cm^{-1} are attributed to the POH deformation modes of the $HOPO_3^{2-}$ units.

The Raman spectrum of taranakite in the 350 to 700 cm^{-1} is reported in Figure 3. This spectral region is where the PO_4^{3-} and $HOPO_3^{2-}$ bending vibrations are found. A series of bands are observed at 595, 615, 636, 648 and 656 cm^{-1}. These bands are attributed to the ν_4 out of plane bending modes of the PO_4 and H_2PO_4 units. The Raman spectrum of crystalline NaH_2PO_4 shows Raman bands at 526, 546 and 618 cm^{-1} (this work). A series of bands are observed at 396, 416, 444, 464, and 489 cm^{-1}. These bands are attributed to the ν_2 PO_4 and H_2PO_4 bending modes. The Raman spectrum of NaH_2PO_4 shows Raman bands at 460 and

482 cm^{-1}. The Raman spectrum in the far wavenumber region are shown in Figure 4. Quite intense bands are found at 155, 188, 223, 271, 304 and 328 cm^{-1}. These bands may be simply described as lattice vibrations.

The infrared spectrum of the Jenolan Caves taranakite is displayed in Figure 5. It should be noted that despite many attempts the Raman spectrum of the OH stretching region could not be obtained with any degree of reliability. Infrared bands are observed at 2838, 3054, 3250, 3374 and 3437 cm^{-1}. These bands are assigned to water stretching vibrations. The position of the bands seems to indicate very strong hydrogen bonding between the water molecules and the phosphate units. The bands at 2701 and 2838 cm^{-1} may be assigned to the OH stretching vibration of the POH units. Another possibility is that the bands are due to NH stretching vibrations of the NH_4^+ ions. The water bending region is shown in Figure 6. A strong infrared band is observed at 1647 cm^{-1} and assigned to the water bending mode. The position of the band suggests the water is involved with strong hydrogen bonding. Other low intensity infrared bands are observed at 1416, 1435 and 1465 cm^{-1}. These latter bands are attributed to HNH bending modes of the NH_4^+ anion. The bands are assigned to the doubly degenerate ν_2 modes.

Mechanism for the formation of taranakite

Bat guano provides a source of phosphate anions. Taranakite $(K,NH_4)Al_3(PO_4)_3(OH)\cdot 9(H_2O)$ is formed on the calcite surfaces. The Al^{3+} ions come from clays in the caves. These cave clays are used for the dating of the cave system. The Al^{3+} ions are released through the action of the phosphoric acids on the cave floor clays. The ammonium ion probably comes from the bat guano. It is likely to be translocated through the cave system through dissolution. The taranakite is formed from the reaction of the ions in solution. The following reaction is suggested:

$$K^+ + NH^{4+} + 6H_2O + 3Al^{3+}(OH)_3 + 3H_3PO_4 + 3H^+ \rightarrow (K,NH_4)Al_3(PO_4)_3(OH)\cdot 9(H_2O)$$

An important concept is pH compatability as well as the being stoichiometrically correct. One of the important considerations for the nucleation and crystallisation of taranakite is the temperature and humidity within the Jenolan Caves. The formation of taranakite requires the permanent presence of water. The temperatures within the caves are quite low and vary only

by a small amount throughout the year. Temperature sensing determines the temperature to vary from 12.8 to 15.6°C. The higher temperatures are only achieved near the cave entrances. The humidity within the caves is high and never goes below 75% relative humidity and the air is often saturated.

CONCLUSIONS

Because of the chemicals found in bat guano, a range of phosphate bearing minerals including taranakite, crandallite, brushite and newberyite may be formed. The presence of taranakite in the Jenolan Caves has been identified by combination of X-ray diffraction, Raman and infrared spectroscopic techniques. Bands attributed to PO_4 and HPO_4 groups are identified.

There is a difference between taking a Raman spectrum and an infrared spectrum. The sample spot size of the Raman spectrometer is around 1 micron. In infrared spectroscopy the measurement size is at best 30 microns. Thus in Raman spectroscopy it is possible to collect data for a pure mineral because that crystal was selected. It is more likely that the infrared spectrum is more likely to collect data for a mixture. This is why of course it is an advantage to run the Raman spectrum. Thus Raman spectroscopy is very effective in determining the presence of taranakite in the deposits of the Jenolan Caves.

Acknowledgements

The financial and infra-structure support of the Queensland University of Technology Chemistry Discipline of the Faculty of Science and Technology is gratefully acknowledged. The Australian Research Council (ARC) is thanked for funding the instrumentation.

References

[1] S. Marincea, D.-G. Dumitras, Neues Jahr. Min.(2003) 127.
[2] D. Moravansky, M. Orvosova, Min.Slov. 39 (2007) 203.
[3] J.W. Murray, R.V. Dietrich, Amer. Min. 41 (1956) 616.
[4] T. Sakae, T. Sudo, Amer. Min. 60 (1975) 331.
[5] J. Sejkora, R. Duda, J. Cejka, J. Ederova, M. Novotna, Min.Slov. 36 (2004) 343.
[6] W.B. White, NSS Bull. 44 (1982) 90.
[7] S. Dick, U. Gossner, A. Weiss, C. Robl, G. Grossmann, G. Ohms, T. Zeiske, Inorg.Chim. Acta 269 (1998) 47.
[8] A. Weiss, U. Gossner, C. Robl, Clays Controlling the Environment, Proceedings of the International Clay Conference, 10th, Adelaide, July 18-23, 1993 (1995) 253.
[9] R.L. Frost, J. Raman Spectrosc. 42 (2011) 540.
[10] R.L. Frost, J. Raman Spectrosc. 42 (2011) 1130.
[11] R.L. Frost, S. Bahfenne, J. Raman Spectrosc. 42 (2011) 219.
[12] R.L. Frost, S. Bahfenne, J. Cejka, J. Sejkora, J. Plasil, S.J. Palmer, E.C. Keeffe, I. Nemec, J. Raman Spectrosc. 42 (2011) 56.
[13] R.L. Frost, J. Cejka, J. Sejkora, J. Plasil, B.J. Reddy, E.C. Keeffe, Spectrochim. Acta, A78 (2011) 494.
[14] R.L. Frost, S.J. Palmer, Spectrochim. Acta, A78 (2011) 1255.
[15] R.L. Frost, S.J. Palmer, Spectrochim. Acta, A78 (2011) 1250.
[16] R.L. Frost, S.J. Palmer, J. Cejka, J. Sejkora, J. Plasil, I. Jebava, E.C. Keeffe, J. Raman Spectrosc. 42 (2011) 825.
[17] R.L. Frost, S.J. Palmer, B.J. Reddy, J. Raman Spectrosc. 42 (2011) 1160.
[18] J. Cejka, J. Sejkora, J. Plasil, S. Bahfenne, S.J. Palmer, R.L. Frost, Spectrochim. Acta, Part A 79 (2011) 1356.
[19] R.L. Frost, S.J. Palmer, Spectrochim. Acta, A78 (2011) 248.
[20] R.L. Frost, S.J. Palmer, Spectrochim. Acta, A79 (2011) 1794.
[21] R.L. Frost, S.J. Palmer, Spectrochim. Acta, A79 (2011) 1215.
[22] R.L. Frost, S.J. Palmer, Spectrochim. Acta, A79 (2011) 1210.
[23] R.L. Frost, S.J. Palmer, R.E. Pogson, Spectrochim. Acta, A79 (2011) 1149.
[24] J.W. Anthony, R.A. Bideaux, K.W. Bladh, M.C. Nichols, Handbook of Mineralogy. Mineral Data Publishing, Tuscon, Arizona, USA, 2000.
[25] A. Filipov, Godishnik na Sofiiskiya Universitet, Geologo-Geografski Fakultet 70 (1979) 287.
[26] S. Fiore, R. Laviano, Amer. Min. 76 (1991) 1722.
[27] T. Maki, N. Kashima, Ganseki Kobutsu Kosho Gakkaishi 72 (1977) 181.
[28] R.L. Frost, W. Martens, P.A. Williams, J.T. Kloprogge, Min. Mag. 66 (2002) 1063.
[29] R.L. Frost, W.N. Martens, T. Kloprogge, P.A. Williams, Neues Jahr. Min. (2002) 481.
[30] R.L. Frost, P.A. Williams, W. Martens, J.T. Kloprogge, P. Leverett, Journal of Raman Spectroscopy 33 (2002) 260.
[31] V.C. Farmer, Mineralogical Society Monograph 4: The Infrared Spectra of Minerals. The Mineralogical Society, London,1974.
[32] C.E. Bamberger, W.R. Busing, G.M. Begun, R.G. Haire, L.C. Ellingboe, J.Solid State Chem. 57 (1985) 248.
[33] B.K. Choi, M.N. Lee, J.J. Kim, J. Raman Spectrosc. 20 (1989) 11.
[34] A. Galy, J. Phys.Radium 12 (1951) 827.

[35] H. Poulet, N. Toupry-Krauzman, Proc. Int. Conf. Raman Spectrosc., 6th 2 (1978) 364.
[36] N. Toupry-Krauzman, H. Poulet, M. Le Postollec, J. Raman Spectrosc. 8 (1979) 115.
[37] F.S. Casciani, R.A. Condrate, Sr., Proceedings - International Congress on Phosphorus Compounds 2nd (1980) 175.

List of Figures

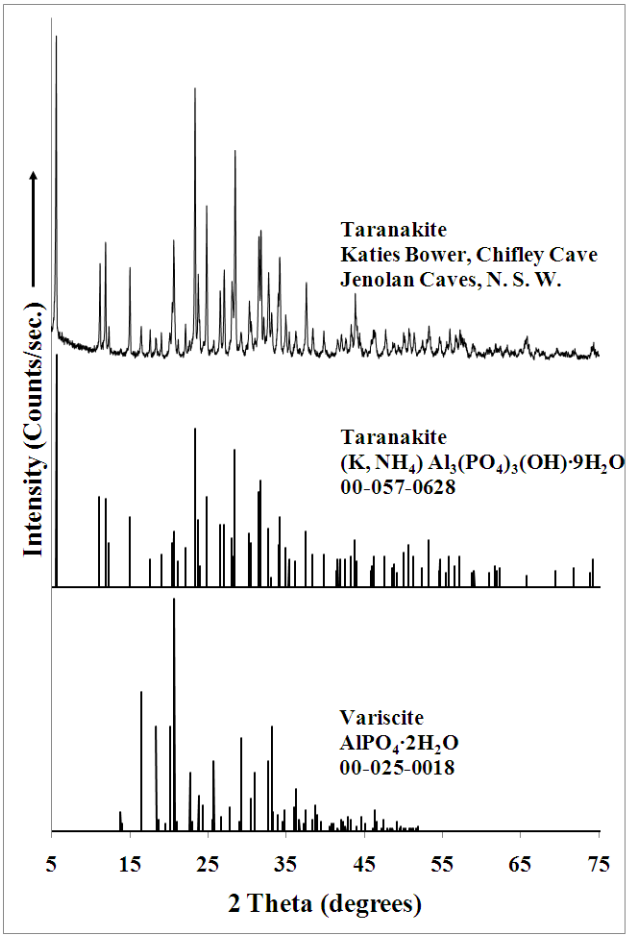
Taranakite
Katies Bower, Chifley Cave
Jenolan Caves, N. S. W.
Taranakite
(K, NH4) Al3(PO4)3(OH)·9H2O
00-057-0628
Variscite
AlPO4·2H2O
00-025-0018
Intensity (Counts/sec.)
5
15
25
35
45
55
65
75
2 Theta (degrees)

Figure 1

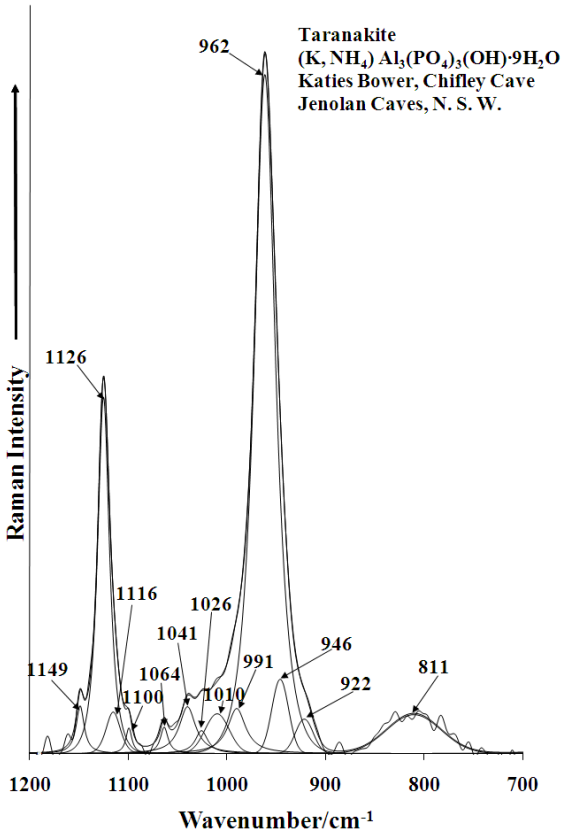

Figure 2a

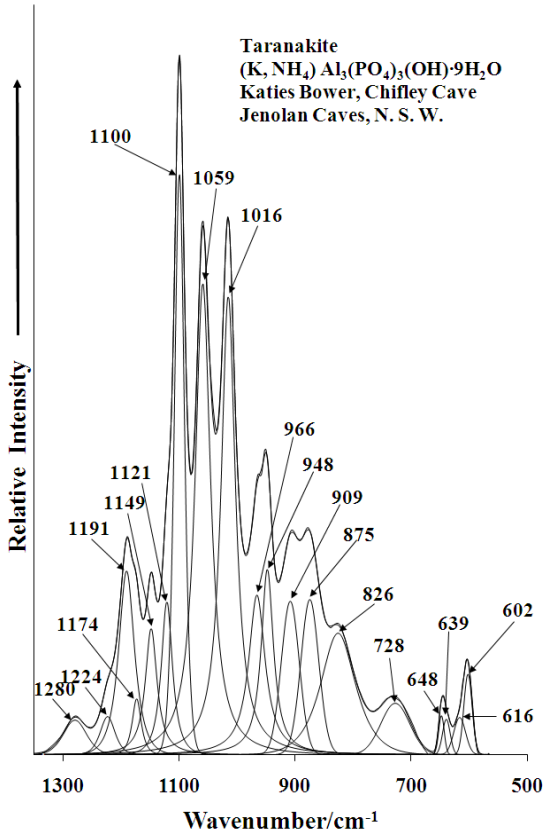

Figure 2b

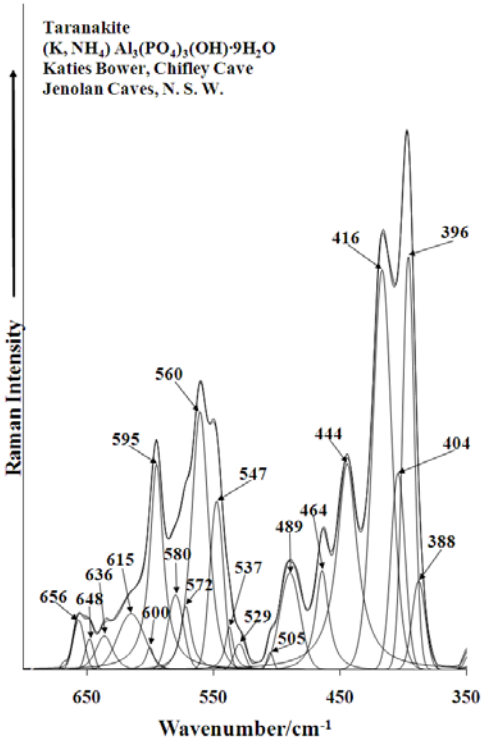
Taranakite
(K, NH4) Al3(PO4)3(OH)·9H2O
Katies Bower, Chifley Cave
Jenolan Caves, N. S. W.
Raman Intensity
416
396
560
595
444
404
547
464
489
388
615
580
537
636
572
656
648
600
529
505
650
550
450
350
Wavenumber/cm-1

Figure 3

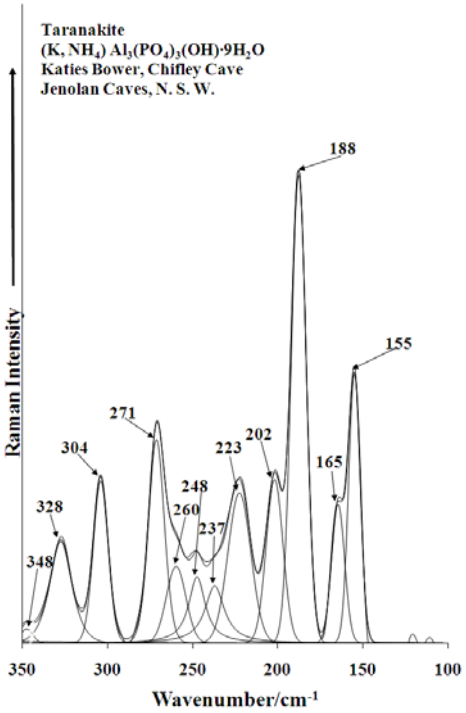
Taranakite
(K, NH4) Al3(PO4)3(OH)·9H2O
Katies Bower, Chifley Cave
Jenolan Caves, N. S. W.
Raman Intensity
188
155
271
304
223
202
165
248
260
237
328
348
350
300
250
200
150
100
Wavenumber/cm-1

Figure 4

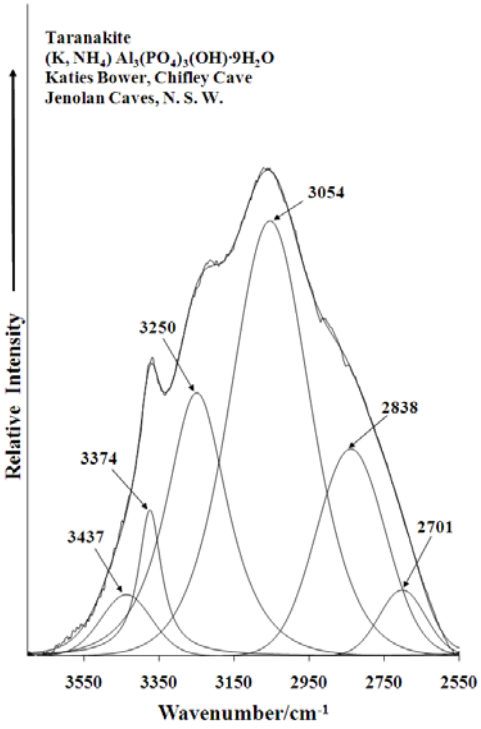
Taranakite
(K, NH4) Al3(PO4)3(OH)·9H2O
Katies Bower, Chifley Cave
Jenolan Caves, N. S. W.
Relative Intensity
3054
3250
2838
3374
2701
3437
3550
3350
3150
2950
2750
2550
Wavenumber/cm-1

Figure 5

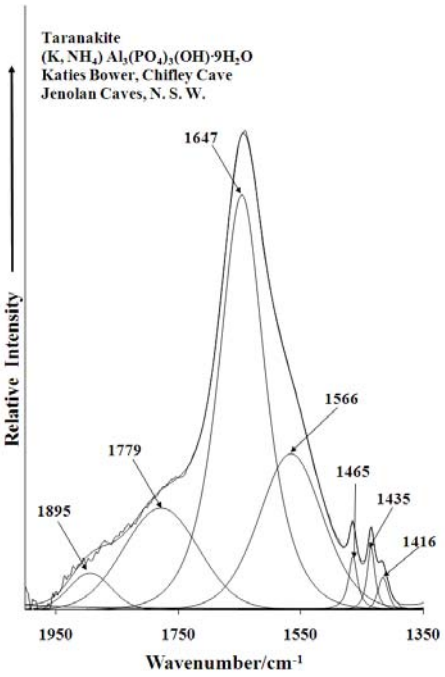
Taranakite
(K, NH4) Al3(PO4)3(OH)·9H2O
Katies Bower, Chifley Cave
Jenolan Caves, N. S. W.
Relative Intensity
1647
1566
1779
1465
1435
1895
1416
1950
1750
1550
1350
Wavenumber/cm-1

Figure 6

	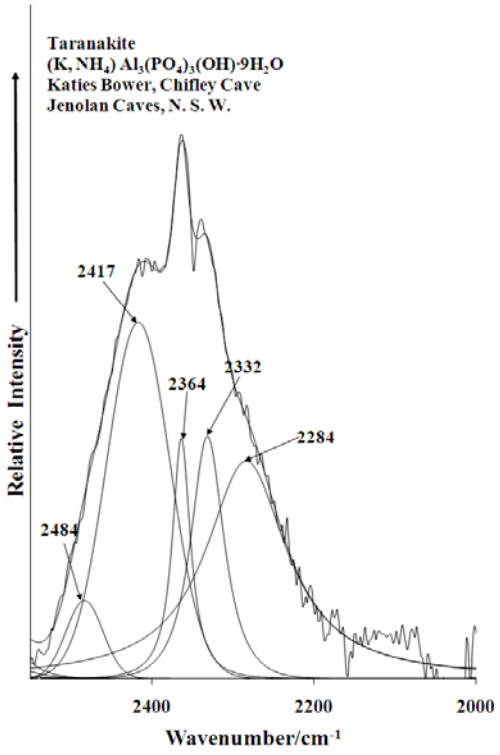 Taranakite (K, NH4) Al3(PO4)3(OH)·9H2O Katies Bower, Chifley Cave Jenolan Caves, N. S. W. Relative Intensity 2417 2364 2332 2284 2484 2400 2200 2000 Wavenumber/cm-1
Figure	**5b**